

Micro-combined heat and power using dual fuel engine and biogas from discontinuous anaerobic digestion

Naim Akkouche^{a,b,*}, Khaled Loubar^b, François Nepveu^a, Mohamed El Amine Kadi^b, Mohand Tazerout^b

^a CEA Tech en Pays de la Loire et Bretagne, Technocampus Océan, 5 rue de l'Halbrane 44340 Bouguenais, France

^b Laboratoire GEPEA, UMR 6144, CNRS, IMT Atlantique-Site de Nantes, Nantes, France

ARTICLE INFO

Keywords:

Micro CHP
Anaerobic digestion
Dual fuel engine
Artificial Neural Network
Cogeneration

ABSTRACT

The modeling of the Micro-CHP unit operating in dual-fuel mode is performed based on experimental results carried out at the laboratory scale. The engine tests were performed on an AVL engine, with a maximum power of 3.5 kW, using conventional diesel as pilot fuel and synthetic biogas as primary fuel. The biogas flow rate is evaluated using the experimental results from the literature, based on the anaerobic digestion in batch reactor of a mixture of 26% of Oat Straw and 74% of Cow Manure, diluted to contain only 4% of volatile solid.

The engine operation was modeled using the Artificial Neuron Network (ANN) method. Experimental engine tests were used as a database for training and validation phases of ANN models. Three different ANN models are developed to model respectively the pilot fuel flow rate, the airflow rate and the exhaust gas temperature. Engine power output, biogas flow rate and biogas methane content were used as the same input layer.

Given that the evolution of the biogas flow evolves along the entire digestion duration (50 days), the simulation work is performed by varying the number of digesters to be used in parallel mode. It is obtained that the optimal operation condition, minimizing the number of digesters and using less than 10% of the energy from diesel fuel, is to use 5 digesters and run the engine under load of 70%. It is concluded that a micro-CHP unit of 1 kWe, requires a dual fuel generator with a nominal power of 1 kWe, five digesters and a daily availability of effluents of 171 kg/day, consisting of 45 kg/day of oat straw and 126 kg/day of cow manure. It can also produce up to 2.45 kW of thermal power from the exhaust.

1. Introduction

Combined Heat and Power (CHP) is an important alternative for minimizing primary energy consumption by optimizing the efficiency of energy conversion units. CHP is also known as cogeneration, which means the simultaneous generation of electricity and heat from a single fuel source. The term Micro-CHP is often associated with systems whose electrical power does not exceed 50 kW [1]. Micro-CHP in farm, where biogas is produced from anaerobic digestion of effluents, has been of increasing interest to livestock farmers in recent years. Biogas is a cleaner and potentially renewable fuel. It consists mainly of methane (CH₄), carbon dioxide (CO₂), small traces of carbon monoxide (CO), hydrogen (H₂), oxygen (O₂) and hydrogen sulphide (H₂S) [2]. In Europe, biogas represented in 2015 around 8% of renewable energy production and the equivalent of 4% of European natural gas consumption. In 2016, the treatment of organic waste by anaerobic digestion is largely done on farms. Among the 269 anaerobic digestion

units installed in France up to 2016, there are nearly 88.5% units are on farms and only 11.5% in centralized units [3].

The most used heat engines in micro-CHP devices are internal combustion engines. Although the use of gaseous fuel is widespread in spark ignition engines, the high CO₂ content of the produced biogas by anaerobic digestion, especially at the beginning of the digestion reaction, disadvantages the use of biogas as a fuel in the internal combustion engines. Indeed, the high CO₂ content in the intake charge has the disadvantage of increasing the specific heat of the gases and reducing the flame propagation speed [4]. It also decreases the energy quality of the fuel and thus increases fuel consumption [5].

Putting existing diesel engines into dual-fuel operating mode, using diesel as pilot fuel and biogas as primary fuel, has both environmental and economic advantages [6]. In fact, Tippayawong et al. [7] that reported long-term utility in this second operating mode shows negligible effects on engine power and efficiency during the first 2000 h run. Beyond this, a little quantity of carbon deposition inside the combustion

* Corresponding author.

E-mail address: naim.akkouche@cea.fr (N. Akkouche).

<https://doi.org/10.1016/j.enconman.2019.112407>

Received 12 September 2019; Received in revised form 11 December 2019; Accepted 12 December 2019

Available online 24 December 2019

0196-8904/ © 2019 Elsevier Ltd. All rights reserved.

Nomenclature

AC	annual consumption
AMFR	average mass flow rates
ANN	artificial neuron network
BDC	bottom dead center
BSFC	brake specific energy consumption
BTE	brake thermal efficiency
CA	crank angle
CCHP	combined cooling, heating, and power
CHP	combined heat and power
CM	cow manure
CI	compression ignition
Cp	specific heat (J/kg.K)
ER	energy ratio
EVC	exhaust valve close (degree)

EVO	exhaust valve open (degree)
\dot{H}	thermal power (W)
IA	injection angle (degree)
IVC	inlet valve close (degree)
IVO	inlet valve open (degree)
LHV	lower heating value (J/kg)
\dot{m}	mass flow rates (kg/s)
MR	mass ratio
MSE	mean square error
OS	oat straw
R^2	regression coefficients
RMSE	root mean square error
RNG	rundum number generation
TDC	top dead center
TS	total solid
VS	volatile solid

chamber was observed [7]. Different techniques were examined to improve the operation of compression ignition (CI) engines in diesel-biogas dual fuel mode such as the use of low levels of substitution [8], preheating of induced air-fuel mixtures [9,10], modifying the pressure and temperature of the initial charge using exhaust gas recirculation process [11,12] and modification of the pilot fuel injection system [13,14].

Biogas is often used as the primary fuel in dual-fuel engines because of its high anti-knock properties compared to other gaseous fuels. With a methane content of up to 65%, its high octane number allows it to have greater knock resistance and better adaptation to engines that generally have higher compression ratios [15]. It was reported that in combined cooling, heating, and power (CCHP) systems, where production of heat, cold and power occur simultaneously from the same primary energy, biogas-diesel dual-fuel mode reduces CO₂ emissions by 24.9% compared to the single production mode [16].

In dual-fuel operating mode and under higher engine loads (above 80%), the brake specific energy consumption (BSFC) is slightly lower than that of conventional diesel mode, whereas the brake thermal efficiency (BTE) in dual-fuel mode is considerably lower than that of diesel mode. On the other hand, under lower engine loads, the lower BTE and the higher BSFC are generally caused by incomplete combustion of the biogas-air mixture due to a poor mixture and a lower temperature in the cylinder [17]. Although the BTE is slightly affected under higher engine loads, it remains largely dependent on CH₄/CO₂ ratio of the biogas composition [18]. Increasing the CH₄ content of the biogas, which raises the heat release rate, leads to a significant increase in the BTE [15,19]. However, the substantial replacement of the pilot fuel with the gaseous fuel causes a remarkable BTE degradation [20]. The gaseous fuel, whose ignition temperature is much higher than the pilot fuel, will act as heat sink during the combustion process. It causes an undesirable increase in the specific heat capacity of the working fluid and consequently, it decreases the combustion temperature [21]. Nathan et al. [22] have shown that above 40% of CO₂ in biogas, the dissociation of CO₂ into O₂ and CO significantly affects the ignition delay.

On the other hand, the lower carbon content of CH₄ compared to petroleum-based diesel reduces the exhaust gases emissions [23]. Several researchers have confirmed that the relative homogeneous charge and the lower cylinder temperature in dual-fuel operating mode have the advantage of significant reduction of NO_x and smoke emissions [21,24,25]. As regards the HC and CO emissions, they are higher when the biogas substitution is high, especially if its percentage of CO₂ is high [26]. With regard to the exhaust gas temperature in the dual-fuel operating mode, it has been shown to be higher than that of the diesel operating mode [27,28].

In micro-CHP on farm, the biogas is produced from anaerobic

digestion of livestock effluents whose the characteristics and composition are very random. Anaerobic co-digestion of livestock effluents and agricultural waste is widely applied in Europe [29,30]. Anaerobic digestion on the farm, which involves the production of biogas from agricultural biomass, is becoming increasingly important as it offers significant environmental benefits and provides an additional source of income for farmers [31]. Livestock effluents in the form of manures (generally semi solid with a high straw content) or slurry (only cattle excrement that is generally liquid) are of interest for anaerobic digestion because of their high potential of biogas production.

Several studies have been conducted to investigate the increased biogas production through anaerobic digestion of livestock effluents [32–35]. The potential of biogas production not only depends on the chemical composition of the effluents, but also on the anaerobic digestion state (solid state, liquid state, pasty state), type of digesters (continuous reactor, semi continuous reactor, batch reactor) and on the operating conditions (digestion temperature, recirculation of percolate ... etc.).

In continuous or semi-continuous anaerobic digestion, the composition and flow rate of biogas leaving the digester are practically constants. Depending on the composition of the effluents and on the operating conditions, the methane content is often between 55 and 65% [36]. The major disadvantage of this pathway is the high investment costs, especially for small power plants. In France, for example, anaerobic digestion plants with electrical power of 35, 170 and 500 kW_e respectively, have the investment costs of 12.5, 5.6 and 5.6 k€/kW_e [37]. A large part of the investment costs is reserved for the biogas storage, its homogenization, sealing systems and security. This is because the biogas must be produced continuously and with a methane content between 55 and 65% to be acceptable in the gas engines. Indeed, a biogas whose low methane content causes flammability and efficiency problems and a biogas whose methane content is too high causes the knocking problems in gas engines.

In the discontinuous digestion process (batch reactor), where the digesters are sized according to the size of the farm and the availability of the effluents, the investment and maintenance costs for the small plants can greatly reduce compared to those of the continuous digestion process. The most problem is that the flow of biogas leaving the digester and its methane content change throughout the anaerobic digestion time, which is often between 40 and 60 days. The purpose of this study is to overcome these constraints and use this pathway to develop on-farm micro-CHP technology. It involves two objectives: The first is to use a dual-fuel engine to use the biogas leaving the digester regardless of its flow and its methane content. It eliminates the need for biogas storage, which significantly reduces investment costs. The second objective is to determine the number of digesters needed to optimize the operation of a micro-CHP unit on the farm. For this purpose, a

simulation work of a micro-CHP unit based on experimental data from laboratory tests was performed. Simulation of the engine operation in dual fuel mode is carried out using artificial neural network (ANN) models. The novelty of the present work is to model and develop a diesel engine map, operating in diesel-biogas dual-fuel mode taking into account the availability of biogas in term of quantity and quality (composition). This expresses that the operation of the engine is very flexible to the number of digesters used for the anaerobic digestion of livestock effluents, which in turn directly influences the primary fuel (biogas) supplied to the engine. In addition, the model makes it possible to minimize the number of digesters so that the biogas produced is directed to the engine without storage. As a result, the pilot fuel remains minimal in accordance with the regulatory limits, making it possible to benefit from the feed-in tariffs of electricity.

ANN is a popular machine learning technique that has been shown its effectiveness in various fields [38]. This form of black-box modelling approach allows the omission of physical knowledge or equations that relate the relationship between the input and corresponding output without the loss of accuracy unlike white and grey box modelling, albeit care must be taken in the selection of appropriate input and outputs to avoid meaningless predictions.

The engine modeling technique using the ANN models is more preferable nowadays because it can identify a complicated and unknown input/output relationship based on experimental data. It has several advantages compared to mathematical engine models (analytical multi-zone models, computational fluid dynamic models and chemical kinetic models) which are very difficult to put into practice because excessive assumptions have been made in constructing the models [39–42]. In addition, these mathematical models depend on several engine-specific parameters, which are generally difficult to estimate or to predefine (inlet valve flow coefficient, kinetic of combustion, local air fuel ratio, local heat loss coefficient...etc.). Furthermore, ANN has a better capability in approximating input–output relationship that polynomial regression models owing to its ability in capturing non-linear behavior of a given system in particular for a large number of measured data [38].

Several studies have been conducted on diesel engine performance and/or emissions modeling using neural network models [39,43–45]. Others have also used this method for performance modeling and emission characteristics, and even the elaboration of the operational maps for engines operating with biodiesel blends [46–48]. Similarly for the modeling of engines operating in dual-fuel mode, researchers are increasingly interested in the use of the ANN method to model the operation, performance, emissions and even develop operational maps for the dual fuel engines [49–51].

Since the modelling of the diesel engine is a regression task, two situations need to be considered. The first situation is that the model output is single dimension, which means that individual model is required for each engine performance output. The other one is with multi-dimension outputs, where one model is already sufficient to predict several engine performance outputs. In order to increase the model accuracy and prevent any parameter from dominating the output values, the data sets are often normalized before training the models [39,52].

This present paper covers three major parts, namely the kinetic production of biogas from anaerobic digestion of livestock effluents, the modeling of dual-fuel engine using the ANN models, and simulation of the micro-CHP unit operating with dual fuel engine and using biogas as primary fuel. The dual fuel engine setup, the pilot fuel characteristics, the ANN models as well as the kinetics production of biogas are briefly introduced in Section 2. The ANN based models were trained and validated using a series of experimental tests, performed with a 3.5 kW dual fuel engine. The engine models outputs are single dimension. The first is to model the pilot fuel flow rate, the second is to model the airflow rate and the third is to model the temperature of the exhaust gas. The instantaneous production of biogas is determined from the

Table 1
Dual-fuel engine specification.

Parameter	Specification
Model	AVL 5402
Type	Four-stroke, CI engine
Bore × Stroke	85 × 90 mm
Compression ratio	17.3
Injection pressure	600 bar
Combustion system	Dual-fuel
Injection system type	Common rail, direct injection
Nozzle hole × diameter	5 × 0.17 mm
Rated power output	3.5 kW at 1500 rpm
IA	7° CA before TDC
IVO	36° CA before TDC
IVC	69° CA before BDC
EVO	76° CA before BDC
EVC	32° CA before TDC

literature where anaerobic digestion of a mixture of oat straw and cow manure was studied and optimized [53]. In Section 3, where the main results are discussed, the engine tests, the validation of the ANN models, as well as the simulation results of the micro-CHP unit, were presented.

2. Materials and methods

2.1. Dual-fuel engine setup

The engine tests were carried out on a single cylinder research engine (AVL 5402), instrumented to control and measure the operating parameters. The main design specifications as well as the technical operating data are given in Table 1.

Under the same operating conditions, including air–fuel ratio, engine speed and engine loads, the performance parameters of this engine, despite being an water-cooled single-cylinder diesel engine, can be projected on a multi-cylinder engine that can be used in a CHP unit. During the tests, the engine speed was kept constant at 1500 rpm, similar on to that of electric power generator, producing electricity at a frequency of 50 Hz. All tests were carried out to develop an engine power ranging between 1.75 and 3.5 kW. The pilot fuel is a conventional diesel, while the primary fuel is a synthetic biogas, consisting of CH₄ and CO₂.

The experimental procedures consists in fixing the biogas methane content and the pilot fuel flow rate and maintaining the desired engine load acting on the biogas flow rate. It consists in varying the CH₄ content of biogas between 20 and 60% and the engine load between 50 and 100% (i.e. engine power outlet between 1.75 and 3.5 kW). The recorded data from each test are the engine power, biogas methane content, biogas flow rate, pilot fuel flow rate, airflow rate, and exhaust gas temperature.

2.2. Fuels characteristics

The flow rate of the synthetic biogas as well as its CH₄ content have been varied to obtain a wide range and to get closer values to the biogas composition resulting directly from the digesters, without using a storage gasometer. The latter is often necessary to balance the flow rate and composition of biogas (50 to 65% CH₄) for subsequent use.

In practice, the biogas characteristics from anaerobic digestion of cattle effluents, such as flow rate and CH₄ content, vary throughout the entire digestion period, which is of the order of two months. In this study, the biogas is synthesized from pressurized bottles. The methane content of the synthesis gas varies from 20 to 60% while its flow rate is adjusted to develop the desired engine load (between 50 and 100 % of full load).

The pilot fuel, which serves as an ignition source for the mixture, is

a conventional fuel consisting of 93% v/v diesel ($C_{20}H_{40}$) and 7% v/v biofuel ($C_{18}H_{36}O_2$). Its density and lower heating value (LHV) are 840 kg/m^3 and 42.8 MJ/kg , respectively.

2.3. Engine parameters modeling

The engine parameters have been modeled using methodology based on Artificial Neural Networks. An ANN is an architecture containing a huge quantity of neurons systematized in different layers and the neurons of one layer are linked to those of another layer of by dint of weights, and it can be prepared or trained to accomplish a specific duty via creating accurate alteration of its linking weights, bias and architecture [43,44].

In this study, ANN based models have been developed in the MATLAB environment using the Neural Network toolbox. The proposed ANN model consist in three discrete ANNs, developed to estimate engine parameters namely pilot fuel flow rate, intake airflow rate and the exhaust gas temperature. Where, ANN1 is used to delineate pilot fuel flow rate, ANN2 is used to delineate intake airflow rate, and ANN3 is used to delineate exhaust gas temperature. Each ANN has one input layer with three variables (engine power, biogas flow rate and its CH_4 content), up to five hidden layer and one output. Fig. 1 illustrates the architecture of the ANN1 model for the pilot fuel flow rate.

The implementation of ANN comprises of three main stages viz. parameter selection, training, and testing. As regard the parameter selection, the input–output data is often processed by normalizing it within a certain range [38,43]. The recorded data from the experimental tests (83 tests) is then normalized and randomly partitioned with respect to training, testing and/or validation. They are divided into two sets of which the first (68 tests) is selected as the training (80%) and validation (20%) dataset, while the second (15 tests) is selected to testing the generalization capability of ANN models. The training dataset is used to train the model and tuning model hyperparameters (weights and biases). The model sees and learns from this data. The validation dataset is used to evaluate a given model, but this is for frequent evaluation. It is used to fine-tune the model hyperparameters. The test dataset provides the gold standard used to evaluate the model. It is only used once a model is completely trained (using the train and validation sets). Since the choice of the test dataset significantly influences the model training, the control random number generation (RNG) function of Matlab software is used to control the random selections of the results and an optimal selection has been made for each model. It consists in choosing the selection that minimizes the RMSE among the 100 different random selections. Normalized parameters such as engine power, biogas flow rate, methane content, pilot fuel flow rate, airflow rate and exhaust gas temperature respectively were obtained by dividing their values by 4 kW, 60 g/min, 100% v/v, 20 g/min, 300 g/min and 600°C .

After selecting the input and output parameters, the key parameters specified prior to any ANN investigation are the number of hidden layers, the number of neurons in the hidden layers, the activation function, as well as the training (learning) algorithms. Since there is no precise rule to determine the number of hidden layers and the number of neurons in the hidden layer, the trial and error method has been applied to find the number of hidden layers and the number of neurons in the hidden layer. In order to decide the most appropriate or best solution a software was developed to design and train the network by varying the number of hidden layers from 1 to 5 and the number of neurons in each hidden layer from 1 to 20 neurons. Fig. 2 illustrates the calculation flowchart for selection data optimization, ANN model design optimization, and ANN model training.

For each design, 250 iterations were performed where the new obtained optimal design is updated. The optimum solution has been selected by minimizing the root mean square error (RMSE), given by Eq. (1). Indeed, various studies have been shown that the application of ANN method in engine performance consists of optimal configurations consisting of using one to two hidden layers whose number of neurons in each layer does not exceed ten [38,43–45].

$$RMSE = \sqrt{\frac{\sum_{i=1}^n (Output_Cal_i - Output_Mes_i)^2}{n}} \quad (1)$$

Where : $Output_Cal_i$ and $Output_Mes_i$ are respectively the i^{th} calculated and measured output values. (n) is the total number of the measured output data.

As shown in Fig. 1, the fully connected layer method is considered, i.e. each neuron is connected to every neuron in the previous layer, and each connection has its own weight. Each neuron of hidden layer is molded by input(s), addition block and activation function followed by the output. The weight is a value that defines the strength of the input connected to the node. A bias controls the magnitude of the input for the activation function, in which the magnitude is increased with a positive bias and vice-versa. The computational model is given by the perceptron model in Fig. 3 [38].

The general expression of the output of the model is

$$u = b + \sum_{i=1}^N w_i x_i \quad (2)$$

The output of the perceptron model is governed by the activation (transfer) function. The hidden layers are governed by the log-sigmoid activation function (logsig) while the output layer is governed by the linear activation function (purelin). The log-sigmoid activation function (Eq. (3)) takes the input (which can be any value between plus and minus infinity) and overwrites the output in the range 0 to 1. The linear activation function (Eq. (4)) leaves the input as it is.

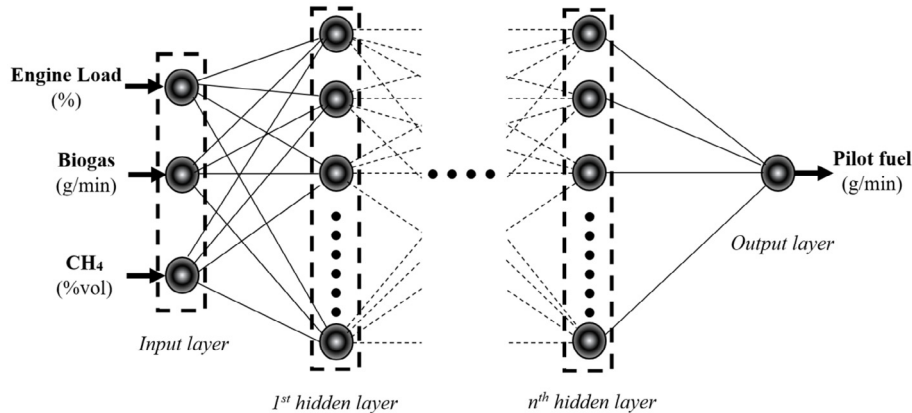


Fig. 1. Configuration of multi hidden layers neural network estimating pilot fuel flow rate.

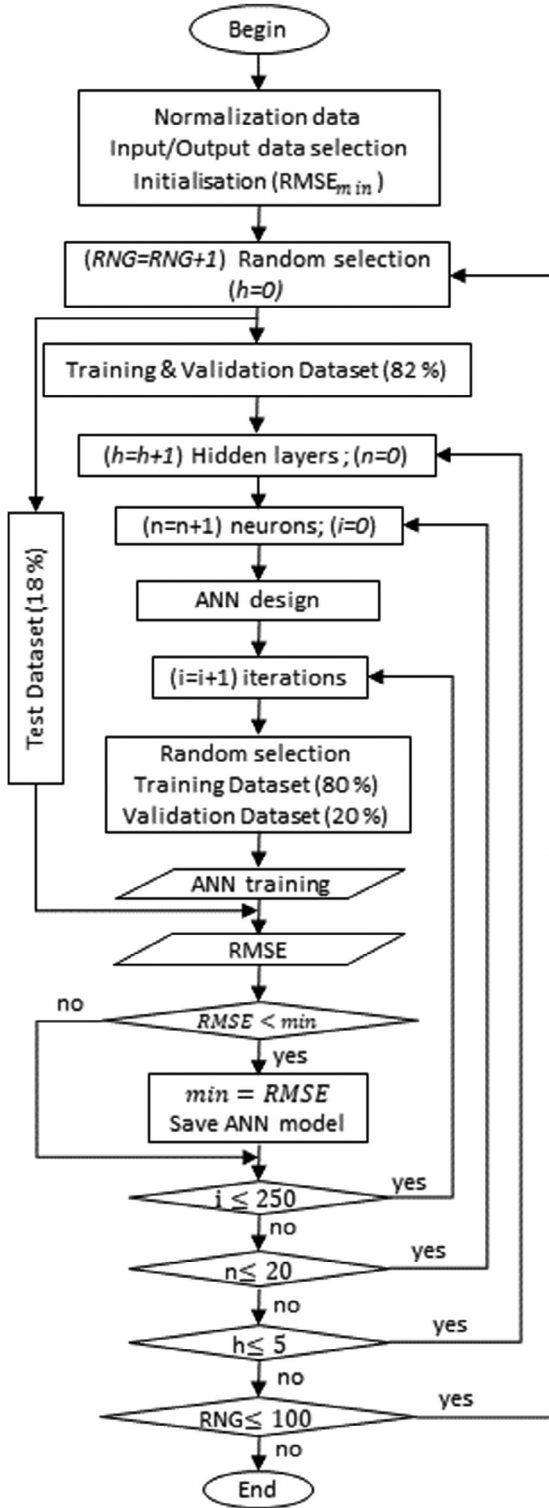


Fig. 2. Flowchart of the design and optimization of the ANN models.

$$f(u) = \frac{1}{1 + e^{-u}} \quad (3)$$

$$f(u) = u \quad (4)$$

The gradient descent with momentum backpropagation training function (traingdm) is used as learning algorithms. It consists in adjusting the network parameters, namely the weights and the biases, by using as a cost function the mean squared error (MSE). The network parameters are backpropagated until the signal is minimized upon a

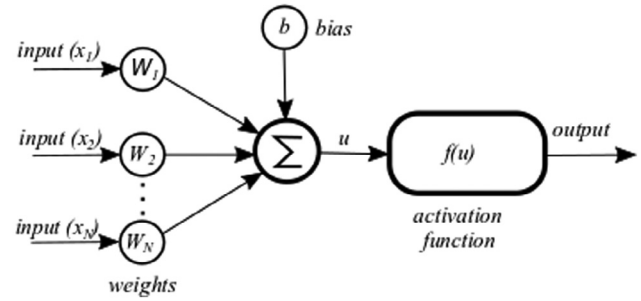


Fig. 3. The perceptron model.

number of training iterations, which is also known as epochs.

2.4. Simulation of biogas production

The evolution of biogas production (flow rate and CH_4 content) from cattle manure effluents were simulated based on previous research works [53]. In fact, the cattle manure effluents, especially in small farms, are often mixed with straw. Zhao et al. [53] investigated the anaerobic co-digestion of oat straw (OS) and cow manure (CM). Their study examined the effects of different percentages of total solid (TS) and the addition of CM on methane production during OS anaerobic digestion. The experiments were conducted at a laboratory scale on 300 ml loads in 500 ml laboratory flasks. The batch tests were carried out in an enclosure maintained at a constant temperature, at $37 \pm 2^\circ\text{C}$, for a maximum of 50 days. This time, usually chosen as hydraulic retention time T95, is considered optimal for the anaerobic digestion reaction. It makes it possible to produce 95% of methane which can be produced when the reaction time is maintained until the completion of the reaction. Table 2 summarizes the OS and CM characteristics.

The produced biogas characteristics, in particular the cumulative production of the main chemical species (CH_4 and CO_2), constituting biogas, divided by the input charge in volatile solids (VS), are represented in Fig. 4. The highest cumulative production of biogas was obtained with a mixture of OS:CM ratio of 2:1 and a TS content of 4%. It was 840 $\text{L}_{\text{biogas}}/\text{kg}_{\text{VS}}$ consisting of 49.6% of CH_4 and 50.4% of CO_2 .

The cumulative production curves summarize the evolution of the total production of biogas per kg of VS of feedstock. This feedstock represents a mixture of 0.889 kg of OS and 2.495 kg of CM, diluted with 29.41 kg of water to contain only 4% of TS. After 50 days of anaerobic digestion, the cumulative production is 840 L of biogas, consisting of 416 L of CH_4 and 424 L of CO_2 .

The shape of the cumulative biogas production curve will be used in simulation work as a flow of biogas from each digester. It allows to model the dual-fuel operating mode without biogas storing gasometer, where the biogas from the anaerobic digesters is directed directly to the intake of the dual-fuel engine (Fig. 5).

Table 2
Characteristics of OS and CM.

Parameter	OS	CM
Total solid (%)	94.73 \pm 0.42	16.8 \pm 0.19
Volatile solid (%)	86.61 \pm 0.66	9.22 \pm 0.08
Cellulose (%)	29.87 \pm 1.14	22.91 \pm 0.28
Hemicellulose (%)	30.12 \pm 1.35	22.85 \pm 0.11
Lignin (%)	5.23 \pm 0.22	8.09 \pm 0.08
Ash (%)	14.36 \pm 0.26	6.32 \pm 0.17
Total carbon (%)	36.35 \pm 0.31	26.27 \pm 0.14
Total nitrogen (%)	0.67 \pm 0.01	1.20 \pm 0.04
Carbon/Nitrogen ratio	54.25	21.89

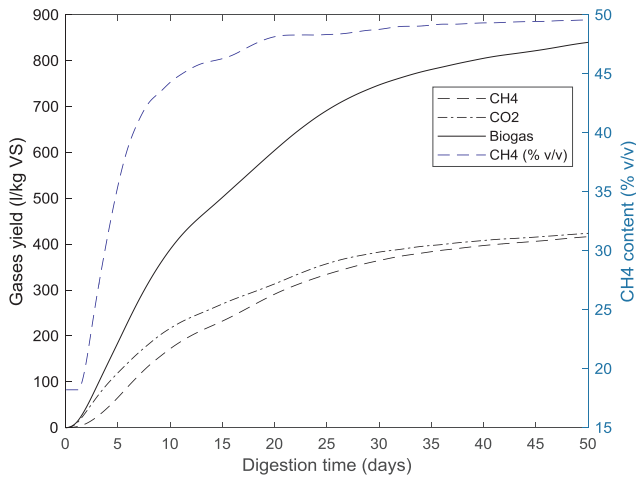


Fig. 4. Cumulative production of biogas from Co-digestion of OS and CM at 37 °C.

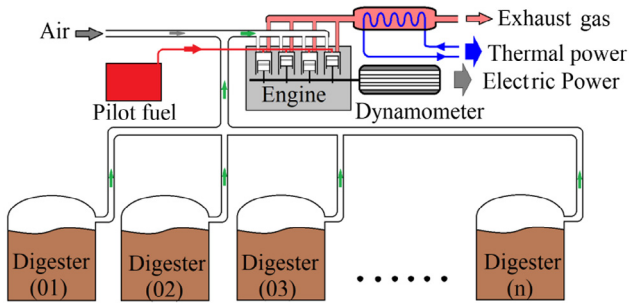


Fig. 5. Schematic of the CHP plant operating with biogas from n digesters.

3. Results and discussion

3.1. Engine tests

The experimental results used to train, validate and test the ANN models are presented in Fig. 6. It summarizes the selected input data (engine power, biogas methane content, biogas flow rate) and the selected output data of the ANN models (pilot fuel flow rate, airflow rate, and exhaust gas temperature).

The training and validation dataset is presented in blue color while the test dataset is presented in red color. It is clear that the optimal selection of the test dataset differs for each model. The optimum choices of the test dataset for models ANN1, ANN2 and ANN3 respectively are obtained using the control random number generation (RNG) of 34, 76 and 68. It is obvious that the choices of the test dataset are different. This is because the physical models that connect the model outputs to their inputs (engine power, biogas methane content and biogas flow rate) are also different.

The results allow us to draw two conclusions: The first is that the chosen experimental procedure makes it possible to scan all the possible cases and to have a very representative experimental set. The second is that the control random selection of the test dataset plays a key role in the ANN modeling. Indeed, uncontrolled random selection risks selecting unrepresentative or undiversified dataset.

3.2. Performances and validation of ANN based models

The models are validated using two criteria namely RMSE and R-squared (R^2). The RMSE is an absolute measure of fit, whereas R-squared is a relative measure of fit. RMSE is a good measure of how accurately the model predicts the response, and it is the most important criterion for fit if the main purpose of the model is prediction. It indicates how close the observed data points are to the model's predicted values. Lower values of RMSE indicate better fit. With regard to R-squared, it has the useful property that its scale is intuitive: it ranges from zero to one, with zero indicating that the proposed model does not

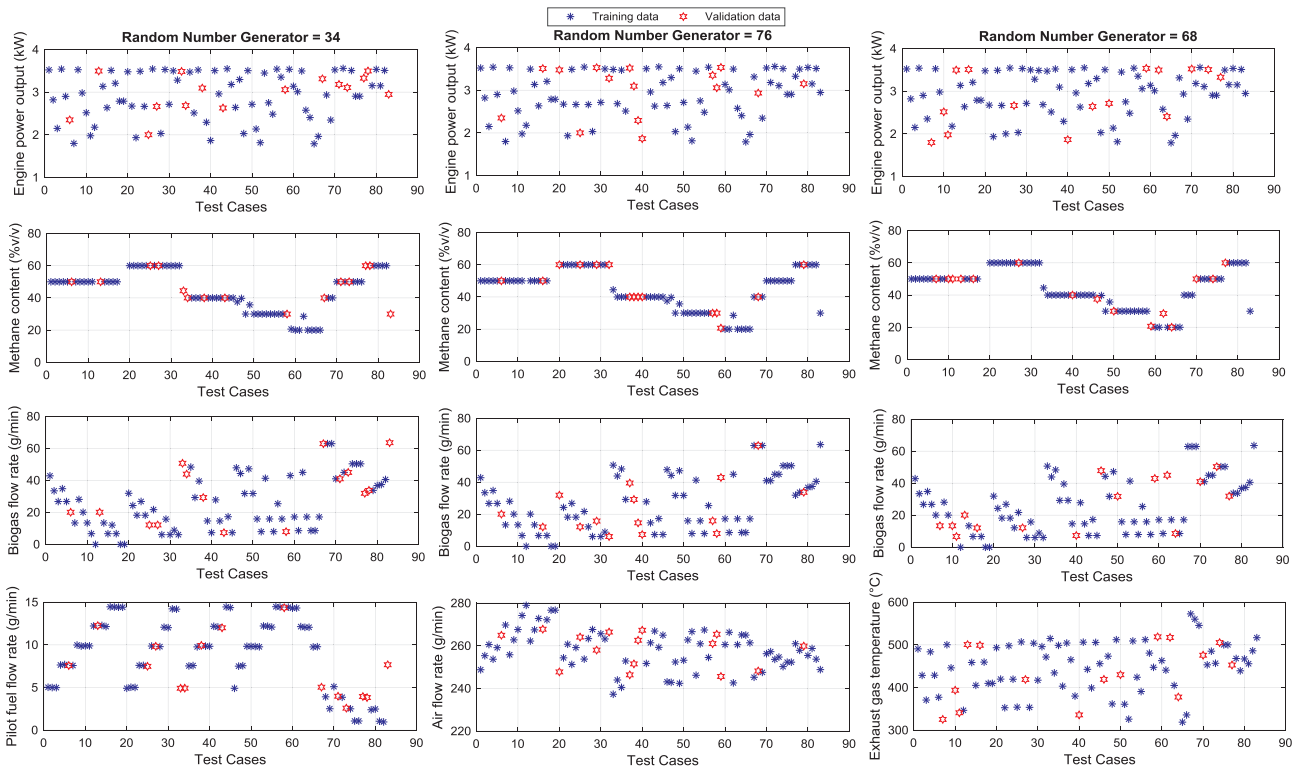


Fig. 6. Experimental tests and the optimal random selection of the training and validation data.

improve prediction over the mean model, and one indicating perfect prediction.

It is found that the optimal configurations of the models ANN1, ANN2 and ANN3 respectively have the RMSE values of 0.58%, 0.34% and 0.62% and the regression coefficients (R^2) values of 0.9993, 0.9858 and 0.9959. The propinquity of the R^2 values to (1) and RMSE values to (0) signifies the accurateness of the ANN based models [43,54]. It reflect that these ANN models give quite satisfactory and acceptable performance. This suggests that the ANN model of the engine is accurate, valid and reliable. The performance graphs for the networks with good agreement between experimental and calculated results are shown in Fig. 7.

The good precision and steadfastness of the ANN based models also reflect the good choice of the inputs parameter selection of the models, such as engine power, biogas methane content and biogas flow rate. Indeed the fact that the engine power depends on the fuels flow rates (pilot and primary fuels) adequately justifies the physical dependence of the ANN1 model output (pilot flow rate) with the engine power, biogas flow rate and biogas methane content. Regarding the physical dependence of the airflow rate (ANN2 model output), it is related to the model inputs through the admitted flow of biogas. Indeed, the intake flow of the engine, naturally aspirated under a constant engine speed (1500 rpm), consists of the sum of two flows, namely the airflow and the biogas flow (biogas flow rate and its methane content). As for the physical dependence of the airflow rate to the engine speed, it is already explained in the physical dependence of the parameters of the ANN1 based model, where the biogas flow rate and the engine speed are physically dependent. For the physical dependence of the ANN3 model parameters, it is evident that the exhaust gas temperature depends on the engine power, biogas flow rate, and biogas methane content (i.e. CH_4 and CO_2 flow rates). In the diesel engine, where under a constant engine speed the volumetric efficiency is practically constant, the variation of the power implies the variation of the air fuel ratio which in turn affects the exhaust temperature. In addition, the variation of the biogas flow and the methane content implies the variation of the CO_2 flow rate, which is an inert gas and therefore its presence decreases the exhaust temperature.

As regards the ANN1 based model, its optimal configuration consists of two hidden layers for which the first comprises five neurons and the second comprises four neurons. Their optimal adjusted network parameters, namely the weights and the biases, are shown in Table 3.

Where, i = input variables, j = Hidden layer neurons, $IW_{j,i}$ = weight to j^{th} neuron of hidden layer from i^{th} input variable, $LW_{j,i}$ = Weight to output layer from j^{th} neuron, $b_{1,j}$ = bias to j^{th} neuron of 1st hidden layer, $b_{2,j}$ = bias to j^{th} neuron of 2nd hidden layer, b_3 = bias to j^{th} neuron of output layer.

For the ANN2 based model, its optimal configuration also consists of two hidden layers for which the first comprises three neurons and the

Table 3

Weight and biases of the ANN 1 based model.

1st Hidden layer : $IW_{j,i}$					$b_{1,j}$
1.5733	-3.2675	-2.6178	-12.4954		4.6390
0.6322	-1.7464	-2.7040	0.1185		-2.5938
-0.0659	-0.2166	-0.3591	0.1678		1.3898
17.0472	63.1983	3.9064	23.0693		33.2631
0.3928	-0.1054	4.9590	-1.5147		-5.7573
2nd hidden layer : $IW_{j,i}$					$b_{2,j}$
-0.1093	-33.2032	-18.4208	-0.0635	-2.2667	12.5516
30.9308	-30.9775	5.0478	-24.3578	-2.6255	-9.9047
110.3573	16.8241	11.4910	-10.4912	-23.9237	11.3550
0.0259	-0.6688	13.4434	0.0250	0.9057	-8.2412
Output hidden layer : $LW_{j,i}$					b_3
-19.1421	0.0824	11.6260	-27.5964		14.6475

Table 4

Weight and biases of the ANN 2 based model.

1st Hidden layer : $IW_{j,i}$					$b_{1,j}$
-0.0045	-2.4101	6.3145	0.0066		-5.4061
0.0022	0.6448	-0.3752	0.0110		-0.3895
-17.4060	62.4664	-20.2027	95.2348		-24.6803
2nd Hidden layer : $IW_{j,i}$					$b_{2,j}$
-53.2753	-3.8107	-1.1256			52.4951
88.1274	175.1971	46.5783			-119.3185
-11.8383	2.2070	-0.1461			6.1280
12.0424	36.1368	-0.5266			-17.2298
-82.8240	-170.4725	-36.7020			113.9552
Output hidden layer : $LW_{j,i}$					b_3
45.7544	41.9136	-9.3538	-78.7266	46.7049	-14.6489

second comprises five neurons. Their optimal adjusted network parameters, namely the weights and the biases, are shown in Table 4.

Likewise, for the ANN3 based model, its optimal configuration consists of two hidden layers for which the first comprises five neurons and the second comprises three neurons. Their optimal adjusted network parameters are shown in Table 5.

3.3. CHP simulation results

It is recalled that the engine used, with a maximum power of 3.5 kW, has been able to consume up to 60 g/min of biogas (Fig. 6). Given that the digesters dump the biogas into a manifold (as shown in Fig. 5), the anaerobic digestion unit will be sized so that the maximum flow rate of biogas in the manifold outlet is 60 g/min.

The instantaneous flow rate of biogas leaving a single digester is determined by deriving the cumulative instantaneous production of the digester, given in Fig. 4. Depending on the number of digesters to be

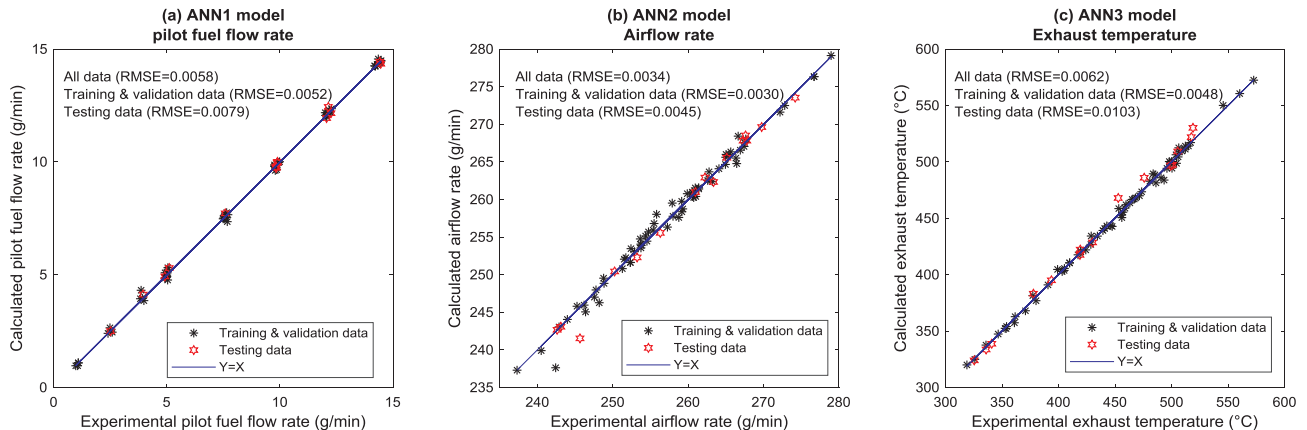


Fig. 7. Experimental versus calculated values for the different recorded parameters.

Table 5
Weight and biases of the ANN 3 based model.

1st Hidden layer: $IW_{j,i}$					$b_{1,j}$
0,1504	0,0775	−1,2412	−1,3139		0,5200
0,5634	−1,0624	4,5390	−2,5093		−1,4359
−0,0130	−0,0178	0,2789	0,2887		−1,6385
1,4895	−30,0325	2,9975	−7,4717		−1,0186
0,4957	−18,3654	15,7180	−17,7499		3,0818
2nd Hidden layer: $IW_{j,i}$					$b_{2,j}$
−0,7228	−0,1800	12,8054	−0,5347	−0,6179	−1,4763
6,9956	2,4618	9,0203	0,6300	1,3695	−9,2359
5,4879	4,2692	−11,4440	0,5861	1,9571	−7,3014
Output hidden layer: $LW_{j,i}$					b_3
16,6370	37,2658	−25,8575			−12,9805

used, the resulted average biogas flow rate and the corresponding digester charge are determined. Fig. 8 shows the evolution of the digester charge as well as the average biogas characteristics (biogas, CH₄ and CO₂ flow rates) as a function of the number of used digesters.

It is observed that when only one digester is used, the amount of effluent (digester charge) is 1187 kg_{VS} (mixture of 1055.2 kg of OS, 2961.6 kg of CM and 34909 kg of water). This charge gradually decreases to reach 355.1 kg_{VS} (mixture of 315.7 kg of OS, 885.97 kg of CM and 10444 kg of water), for each digester, when 10 digesters are used.

It can be noted that the average biogas flow rate increases as the number of digesters increases. This is because the fluctuation of the biogas flow rate decreases while increasing the number of digesters. Indeed, when using two digesters, for example, the loading of the digesters takes place every 25 days. i.e. while the second digester has reached its 25th day of digestion, the first digester has reached its end of digestion (50th day) so it will charge again. On the other hand, when using ten digesters, for example, the digesters are loaded every 5 days. i.e. while the tenth digester has reached its 5th day of digestion, the first digester has reached its end of digestion (50th day). This reduction in the loading time actually has two advantages: the first is to reduce the fluctuation of the flow and the composition of the biogas, the second reduces the storage time of the effluents, which prevents the loss of the methane production yield of the effluents.

Fig. 9.a shows the instantaneous production of biogas flow over a period of 100 days. In the case of a single digester, the fluctuation of the biogas flow rate is between 2 and 60 g/min. Fluctuations are reduced and range between 38 and 60 g/min when the number of digesters exceeds 5. The biogas flow rate becomes less fluctuating. In addition, the biogas methane content (Fig. 9.b), which varies between 18 and 50% when a single digester is considered, quickly becomes stable, between 46 and 49%, as soon as two digesters have been considered.

This biogas, whose flow rate and CH₄ content vary over time, serves as the primary fuel for the operation of the 3.5 kW power engine in dual fuel mode. This involves the variation of the associated pilot fuel flow rate that will be injected into the engine cylinder to develop the desired engine load. Fig. 9-c to 9-f show the effect of the number of digesters as well as the evolution of the pilot fuel flow rate associated with biogas flow rate as a function of the engine load (50, 70, 80 and 100%).

Using these simulation results (Fig. 8 and Fig. 9), the performance of the dual fuel CHP plant will be evaluated on an annual basis (8760 h). Fig. 10 illustrates the average annual pilot fuel flow rate as well as the pilot fuel mass ratio as a function of the engine load and the number of digesters. The pilot fuel mass ratio is given by the following equation:

$$MR_{pilotfuel} = \frac{AMFR_{pilotfuel}}{AMFR_{pilotfuel} + AMFR_{biogas}} \quad (5)$$

Where $AMFR_{pilotfuel}$ and $AMFR_{biogas}$ are the average mass flow rates for pilot fuel and biogas respectively. They are determined as the ratio of annual consumption of the considered fuel to the elapsed time of digestion. They are given by the following equations:

$$AMFR_{pilotfuel} = \frac{AC_{pilotfuel}}{\text{annualldigestiontime}} \quad (6)$$

$$AMFR_{biogas} = \frac{AC_{biogas}}{\text{annualldigestiontime}} \quad (7)$$

Where $AC_{pilotfuel}$ and AC_{biogas} are the annual consumptions of pilot fuel and biogas respectively, calculated by integrating their flow rate curves throughout the digestion time.

The result shows that for a lower number of digesters, the average pilot fuel flow rate increases quickly with respect to the engine load. In the case of a single digester, for example, the pilot fuel flow rate increases from about 7 to 13 g/min when the engine load increases from about 50 to 100%. This is because the biogas flow rate and its methane content show a significant fluctuation. The effect of the number of digesters becomes unimportant from 6 digesters, where the pilot fuel flow rate goes from about 1 to 3.7 g/min when the engine load goes from 50 to 100%. With regard to the mass fraction of the pilot fuel (Fig. 10.b), and under a given engine load, it decreases by increasing the number of digesters so that it becomes negligible when the number of digesters becomes greater than four digesters. This is the consequence of the flow rate and methane content of biogas becoming stable.

One of the limiting factors for the development of micro-CHP technology with dual fuel is the use of diesel fuel as a pilot fuel. The regulated tariffs for electricity from renewable sources generally requires limited consumption of fossil fuels for the operation of the CHP plants. For instance, in France, the current regulation imposes that the annual fossil energy consumption rate should not exceed 10% of the primary energy used in the diesel-biogas CHP plants [55]. Fig. 11 shows the average energy ratio of the pilot fuel ($ER_{pilotfuel}$) as well as the engine efficiency as a function of the engine load and the number of digesters. These two parameters are given by the following equations:

$$ER_{pilotfuel} = 100 * \frac{AMFR_{pilotfuel} LHV_{pilotfuel}}{AMFR_{pilotfuel} LHV_{pilotfuel} + AMFR_{biogas} LHV_{biogas}} \quad (8)$$

$$\text{Engineefficiency} = 100 \frac{\text{Enginepoweroutput}}{AMFR_{pilotfuel} LHV_{pilotfuel} + AMFR_{biogas} LHV_{biogas}} \quad (9)$$

where $LHV_{pilotfuel} = 42.42 \text{ MJ/kg}$ is the lower heating value of pilot fuel and LHV_{biogas} is the lower heating value of biogas. The latter is calculated according to the methane content of biogas.

Regarding the engine efficiency, it increases proportionally with the engine loads. In addition, for a constant engine load, the increase in the number of digesters implies a slight decrease in engine efficiency. For a

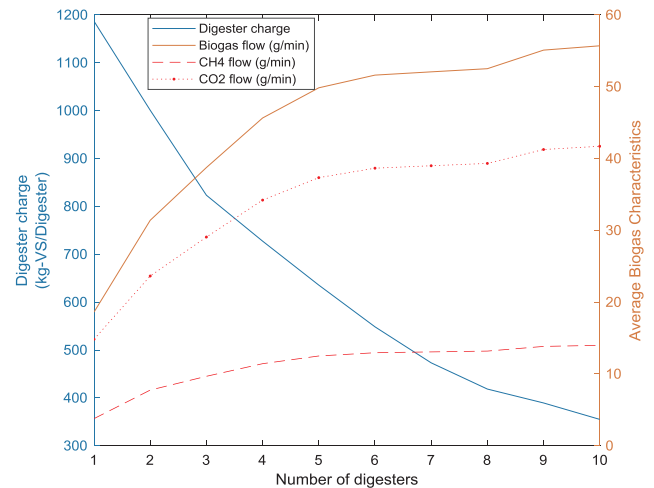


Fig. 8. Digester charge and characteristics of the produced biogas versus number of digester to produce a biogas flow rate whose maximum is 60 g/min.

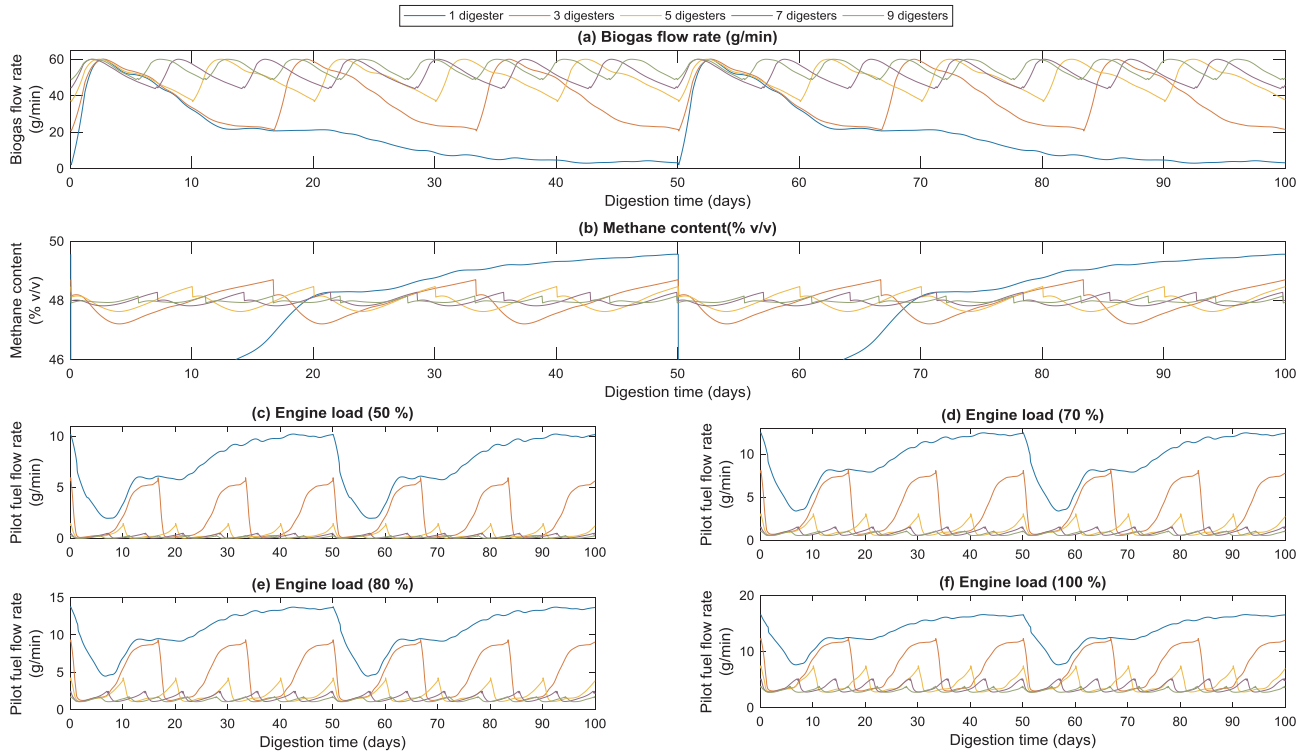


Fig. 9. Biogas flow rate and the corresponding pilot fuel flow rate for different engine power outputs.

load of 70%, for example, the engine efficiency goes from about 25% when a single digester is considered to about 20% when the number of digesters is 10. This is because increasing the number of digesters induces an increase in the biogas flow rate (Fig. 8), which causes a decrease in the pilot fuel flow rate (Fig. 10-a) at a constant engine load. In fact, several researchers reported that increasing the amount of biogas in a dual fuel engine at the expense of pilot fuel involves the reduction of engine efficiency [4,8,56,57]. On the other hand, the pilot fuel energy ratio, shown in Fig. 11-b, decreases while increasing the number of digesters. It is only from 4 digesters that the average pilot energy ratio is less than 10% which complies with French regulation. For operation under an engine load equal to 70%, the number of five digesters can be optimal. In addition to these regulation limits, such as thermal efficiency, pollutant emissions, engine aging and maintenance costs, the

technical limits has also proven that operation under partial loads is recommended. Akkouché et al. [42] have already proved that the indicated thermal efficiency obtained in dual fuel operation is almost similar for partial loads greater than 70%. Finally, this partial load, which represents 70% of the maximum engine power, actually represents a nominal power of 2.45 kW.

For instance, in the case of five digesters, the digester charging period, given as the digestion time (50 days) divided by the number of digesters (5 digesters), is 10 days. Each digester charge is then equal to 635.6 kg_{vs} (Fig. 8) leading to a total inlet charge of 20844 kg (565 kg of OS, 1586 kg of CM and 18693 kg of water). It provides an average biogas flow rate of 50 g/min, consisting of 48% v/v of average methane content (Fig. 8).

In summary, a micro-CHP unit of 1 kw (shaft power) require a dual

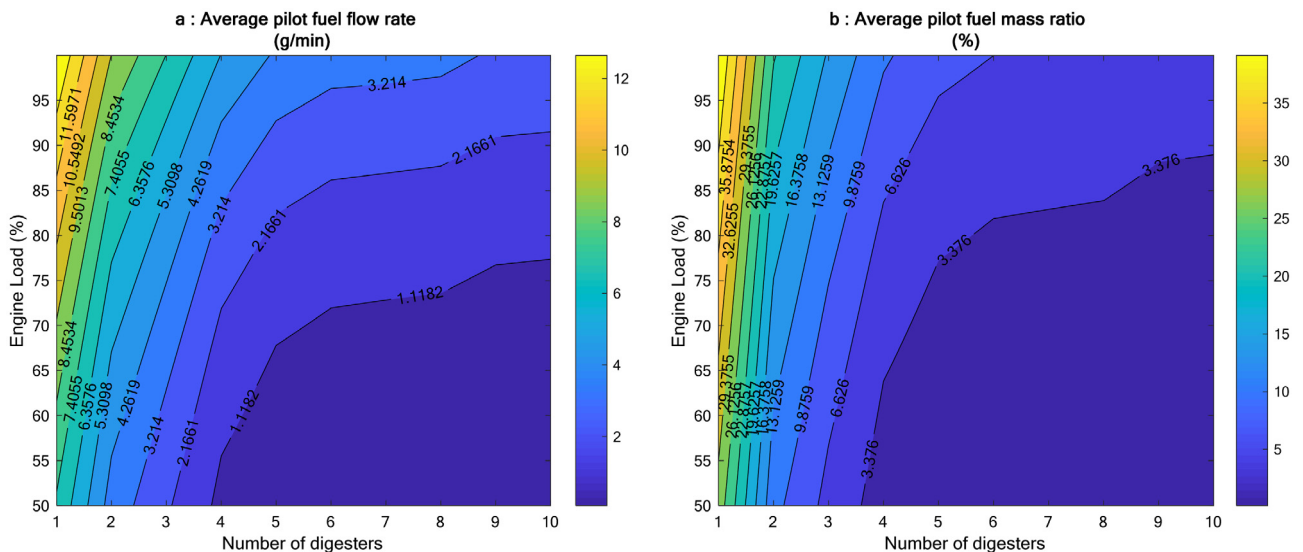


Fig. 10. Average annual fuel consumption versus engine load and number of digesters. a) Average pilot fuel mass flow rate. b) Average pilot fuel mass ratio.

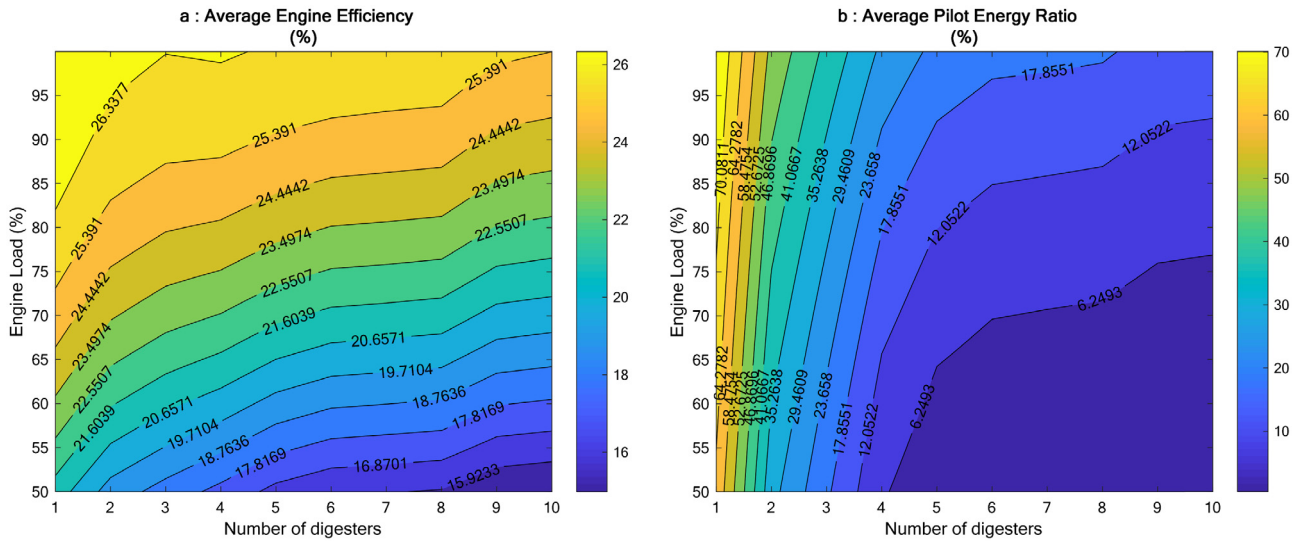


Fig. 11. Engine efficiency and energy ratio versus engine load and number of digesters.

fuel engine generator whose nominal shaft power is 1 kW, five digesters and a daily availability of effluents of 171 kg/day, consisting of 45 kg/day of OS and 126 kg/day on CM.

Since the thermal power of the CHP plant depends on the heat exchanger efficiencies as well as the temperature of the cold source, the study is limited to the estimation of the power heat output available in the exhaust gases. In order to estimate the thermal power, it is necessary to determine the mass flow rate of the exhaust gases, their temperature and their specific heat. As regard to the mass flow rate of the exhaust gases, it is given as the sum of input mass flow rates, such as biogas flow rate, pilot fuel flow rate and airflow rate admitted into the cylinder. The latter is determined using the ANN2 based model. It allows determining the required airflow rate according to the engine load and the number of digesters.

Using ANN3 based model, simulation results show that the annual average airflow rate range from 232 to 260 g/min. This is due to the dependence of the airflow rate with respect to the biogas flow rate, admitted into the engine through its intake manifold. In addition, the fact that the engine speed is constant does not imply that the airflow rate must be constant. Indeed, the airflow admitted into the cylinder

depends on the flow of the biogas injected into the intake duct, and which takes part in the total intake flow sucked by the engine. Various studies have already found this dependence of intake flows, which sometimes results in the variation of the total air fuel ratio [58,59].

Regarding the exhaust temperature, it is determined using the ANN3 based model. Fig. 12a illustrates the average annual exhaust gas temperature as a function of engine load and number of digesters. It is in the range of 340 and 540 °C. Unlike water-cooled engines, where some of the exhaust energy is absorbed in the engine cylinder head, the temperature of the exhaust is often higher. It varies according to the engine load and the air fuel ration [59]. Its increase with the number of digesters is due to the fact that the latter favors the use of biogas at the expense of the pilot fuel. The relatively high presence of biogas flow rate leads to a decrease in the airflow rate, which in turn favors the raising of the exhaust temperature. In fact, the high presence of air (or the lower air-fuel ratios) implies the reduction of the quantity of air in excess, which absorbs a quantity of heat released by the combustion of the fuels.

A reciprocating internal combustion engine CHP system can provide total efficiency (electrical power and thermal energy) of up to 80%

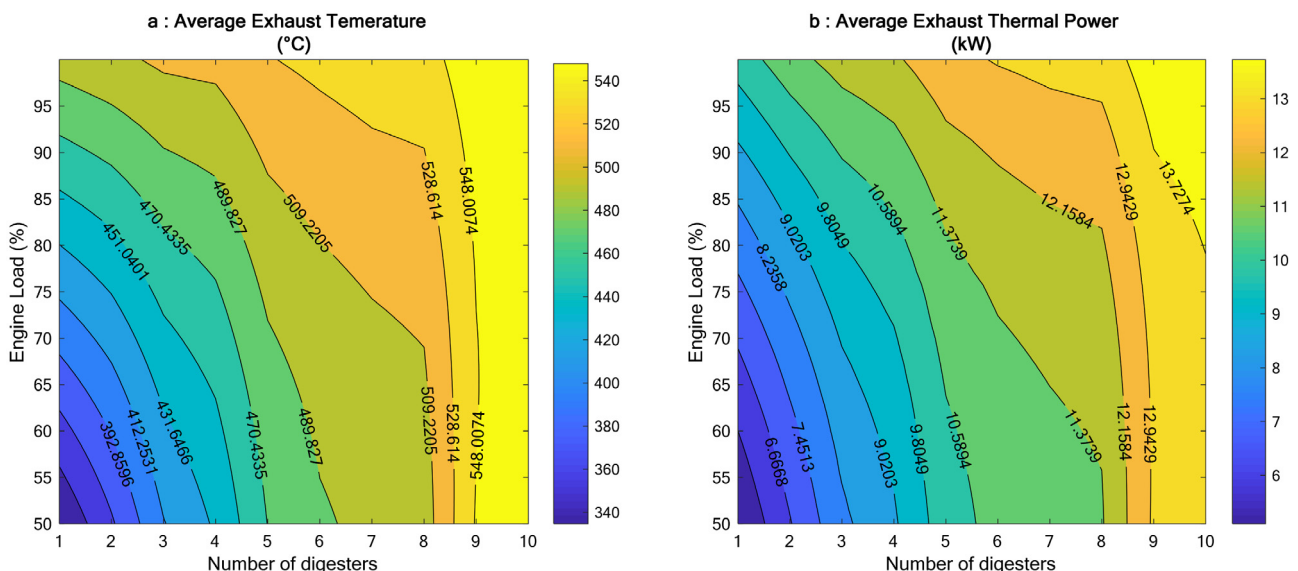


Fig. 12. Exhaust gas temperature and the thermal power output versus engine load and number of digester.

[62]. The heat generated from the engine can be used for numerous purposes such as space heating, cooling, domestic hotwater and other processes of energy recovery from waste such as pyrolysis, gasification, *trans*-esterification, anaerobic digestion, ...etc.

To properly estimate the thermal power of exhaust gases, it is necessary to determine their specific heat according to their chemical composition. Under the assumption of actual complete combustion, the exhaust gas consists mainly of H_2O , CO_2 , N_2 and O_2 . The presence of O_2 on the one hand and the non-presence of the unburned species (CO , HTC , and NO_x) on the other hand imply that the real combustion is considered. The estimation of the CO_2 and H_2O flow rates are determined using the complete combustion of the pilot and primary fuels while the estimation of N_2 and O_2 flow rates are determined taking into account the airflow rate sucked by the engine. Finally, this assumption makes it possible to neglect the presence of the unburned species, which are evaluated in ppm range in the exhaust gases [22,60], and consequently, their presence does not affect the specific heat of the exhaust gases. Therefore, the mass fraction of each species in the exhaust gases is calculated as a function of the biogas flow rate, its methane content, the pilot fuel flow rate and the airflow rate.

The specific heat of each chemical species is given by a correlation as a function of temperature [61]. The specific heat of the exhaust gases ($C_{P_{Exhaust_Gas}}$) is then determined using Eq. (10).

$$C_{P_{Exhaust_Gas}}(T) = x_{H_2O}C_{P_{H_2O}}(T) + x_{CO_2}C_{P_{CO_2}}(T) + x_{N_2}C_{P_{N_2}}(T) + x_{O_2}C_{P_{O_2}}(T) \quad (10)$$

where $C_{P_{H_2O}}(T)$, $C_{P_{CO_2}}(T)$, $C_{P_{N_2}}(T)$, $C_{P_{O_2}}(T)$ are the specific heats in [J/kg.K] of H_2O , CO_2 , N_2 and O_2 respectively. x_{H_2O} , x_{CO_2} , x_{N_2} , x_{O_2} are the corresponding mass fractions of these species in the exhaust gases.

In this study, where the engine is used without the exhaust exchanger, the thermal power of the CHP is expressed by the thermal power available in the exhaust gas at the engine output. It is determined using Eq. (11).

$$\dot{H}_{Exhaust_Gas} = \dot{m}_{Exhaust_Gas} * C_{P_{Exhaust_Gas}} * T_{Exhaust_Gas} \quad (11)$$

where $\dot{m}_{Exhaust_Gas}$ is the mass flow rates of exhaust gas. $T_{Exhaust_Gas}$ is the temperature of exhaust gases in [°C] just at the outlet of the engine combustion chamber (exhaust manifold). Simulation results using ANN3 based model led to evaluate the average thermal power contained in the exhaust gases. Fig. 12b illustrates the evolution of thermal power of exhaust gases as a function of the engine load and the number of digesters. It shows that the thermal power available in the exhaust gas is between 5 and 13 kW. Since the thermal power of the CHP unit is given by the thermal power which is actually recovered, it will be estimated by multiplying the results of the Fig. 12b by the efficiency of the heat exchanger used in the CHP unit. A similar assumption is already used by Teymoori et al. [63] developed a case study applied to an animal farm, covering the technical and economic aspects of biogas production using manure from livestock to replace fossil fuel used for heat and electricity generation. They estimated the thermal power of the CHP plant based on the assumption of constant thermal efficiency, which is estimated at 65% of the primary power.

For the above cited example where a CHP unit consisting of 5 digesters and an engine operating under load of 70% is considered, the thermal power available in the exhaust gas is about 10 kW. In the field of combined heat and power, the used heat exchangers can recover up to 60% of the thermal power contained in the exhaust gases. Indeed, similar percentages have been obtained experimentally by running an 8 kWe cogeneration unit (ecoGEN-08AH) [64] in dual fuel operation mode.

In summary, based on these assumptions, the 1 kWe micro-CHP unit (shaft power), requiring a generator with a nominal electric power of 1 kW, can produce up to 2.45 kW of thermal power.

4. Conclusion

Mico-CHP on farm, where electricity and heat are produced from the anaerobic digestion of farm effluents, is increasingly the focus of many researchers. Dual-fuel engines are known for their flexibility in biogas composition, which varies throughout the duration of the anaerobic digestion reaction. The modeling of the micro-CHP unit operating in dual-fuel mode is carried out on the basis of experimental results carried out at the laboratory scale. The engine tests were carried out on an AVL engine with a maximum power of 3.5 kW, operating in dual fuel mode. The biogas flow rate is evaluated using experimental results from the literature based on anaerobic co-digestion of mixture of oat straw and cow manure.

The engine parameters have been modeled using methodology based on Artificial Neural Networks. Three ANN based models are developed to estimate engine parameters namely pilot fuel flow rate, intake airflow rate and the exhaust gas temperature. The inputs of the ANN based models are engine power, biogas flow rate, and biogas methane content. The ANN based models have been shown to provide quite satisfactory and acceptable performance. Their RMSE is between 0.34% and 0.62% and their R-squared is between 0.99 and 1. Each of them consists of two fully connected hidden layers. The ANN1 which models the pilot fuel flow rate includes five neurons in its first hidden layer and four neurons in its second hidden layer. The ANN2 which models the airflow rate includes three neurons in its first hidden layer and five neurons in its second hidden layer. The ANN3 which models the exhaust temperature includes five neurons in its first hidden layer and three neurons in its second hidden layer.

The effect of the number of digesters on the biogas characteristics is studied and the optimal CHP conception, allowing the use of only 10% of the primary energy from the pilot fuel, is CHP unit consisting of 5 digesters and dual fuel engine whose a nominal load equal to 70% of its maximum load. A micro-CHP unit of 1 kWe, requires a dual fuel generator with a nominal power of 1 kW, five digesters and a daily availability of effluents of 171 kg/day, consisting of 45 kg/day of oat straw and 126 kg/day of cow manure. It can also recover up to 2.45 kW of thermal power from the exhaust gases.

Works using a truly micro-CHP model, operating in diesel-biogas dual-fuel mode and equipped with an exhaust exchanger must be carried out. It is necessary to optimize its operation by acting on two parameters: The first is to improve the efficiency of the engine during operation in dual fuel mode. Indeed, the lower air-fuel equivalence ratio of diesel engines often involves unburned methane in the exhaust, which reduces the efficiency of dual-fuel engines. The second is to optimize the thermal power of the CHP unit by maximizing heat recovery from the exhaust and the heat recovery from the engine jacket.

Declaration of Competing Interest

The authors declare that they have no known competing financial interests or personal relationships that could have appeared to influence the work reported in this paper.

Acknowledgements

We thank Dr. Pierre DERIAN and Dr. Anthony MOURAUD from the CEA Tech en Pays de la Loire for their kind assistance into the simulation software, especially in the application of the neuron network method to model the operation of the engine in dual fuel mode.

References

- [1] Quintana SH, Castaño Mesa ES, Bedoya ID. DECOG – A dual fuel engine micro-cogeneration model: development and calibration. *Appl Therm Eng* 2019;151:272–82. <https://doi.org/10.1016/j.applthermaleng.2019.02.008>.
- [2] Jingura RM, Matengaifa R. Optimization of biogas production by anaerobic

- digestion for sustainable energy development in Zimbabwe. *Renew Sustain Energy Rev* 2009;13:1116–20. <https://doi.org/10.1016/j.rser.2007.06.015>.
- [3] Chaleur issue de la méthanisation de réelles oppor.pdf n.d.
- [4] Bedoya ID, Arrieta AA, Cadavid FJ. Effects of mixing system and pilot fuel quality on diesel-biogas dual fuel engine performance. *Bioresour Technol* 2009;100:6624–9. <https://doi.org/10.1016/j.biortech.2009.07.052>.
- [5] Makareviciene V, Sendzikiene E, Pukalskas S, Rimkus A, Vegneris R. Performance and emission characteristics of biogas used in diesel engine operation. *Energy Convers Manage* 2013;75:224–33. <https://doi.org/10.1016/j.enconman.2013.06.012>.
- [6] Roshia P, Dhir A, Mohapatra SK. Influence of gaseous fuel induction on the various engine characteristics of a dual fuel compression ignition engine: a review. *Renew Sustain Energy Rev* 2018;82:3333–49. <https://doi.org/10.1016/j.rser.2017.10.055>.
- [7] Tippayawong N, Promwungkwa A, Rerkriangkrai P. Long-term operation of a small biogas/diesel dual-fuel engine for on-farm electricity generation. *Biosyst Eng* 2007;98:26–32. <https://doi.org/10.1016/j.biosystemseng.2007.06.013>.
- [8] Abd-Alla GH, Soliman HA, Badr OA, Abd-Rabbo MF. Effect of pilot fuel quantity on the performance of a dual fuel engine. *Energy Conversion* 2000;14.
- [9] Abd-Alla GH, Soliman HA, Badr OA, Abd-Rabbo MF. Effects of diluent admissions and intake air temperature in exhaust gas recirculation on the emissions of an indirect injection dual fuel engine. *Energy Convers Manage* 2001;13.
- [10] Poonia MP, Ramesh A, Gaur RR. Experimental Investigation of the Factors Affecting the Performance of a LPG - Diesel Dual Fuel Engine, SAE International; 1999. <https://doi.org/10.4271/1999-01-1123>.
- [11] Selim MYE. Effect of exhaust gas recirculation on some combustion characteristics of dual fuel engine. *Energy Convers Manage* 2003;15.
- [12] Wong YK, Karim GA. An Analytical Examination of the Effects of Exhaust Gas Recirculation on the Compression Ignition Process of Engines Fueled with Gaseous Fuels, SAE International; 1996. <https://doi.org/10.4271/961936>.
- [13] Sahoo BB, Sahoo N, Saha UK. Effect of engine parameters and type of gaseous fuel on the performance of dual-fuel gas diesel engines—A critical review. *Renew Sustain Energy Rev* 2009;13:1151–84. <https://doi.org/10.1016/j.rser.2008.08.003>.
- [14] Nwafor OMI. Effect of advanced injection timing on emission characteristics of diesel engine running on natural gas. *Renewable Energy* 2007;32:2361–8. <https://doi.org/10.1016/j.renene.2006.12.006>.
- [15] Crookes RJ. Comparative bio-fuel performance in internal combustion engines. *Biomass Bioenergy* 2006;30:461–8. <https://doi.org/10.1016/j.biombioe.2005.11.022>.
- [16] Cacia K, Olmos-Villalba L, Herrera B, Gallego A. Experimental evaluation of a diesel-biogas dual fuel engine operated on micro-trigeneration system for power, drying and cooling. *Appl Therm Eng* 2016;100:762–7. <https://doi.org/10.1016/j.applthermaleng.2016.02.067>.
- [17] Yoon SH, Lee CS. Experimental investigation on the combustion and exhaust emission characteristics of biogas–biodiesel dual-fuel combustion in a CI engine. *Fuel Process Technol* 2011;92:992–1000. <https://doi.org/10.1016/j.fuproc.2010.12.021>.
- [18] Luitjen CCM, Kerkhof E. Jatropha oil and biogas in a dual fuel CI engine for rural electrification. *Energy Convers Manage* 2011;52:1426–38. <https://doi.org/10.1016/j.enconman.2010.10.005>.
- [19] Jiang C, Liu T, Zhong J. Study on compressed biogas and its application to the compression ignition dual-fuel engine. *Biomass London* 1989;20:53–9.
- [20] Duc PM, Wattanavichien K. Study on biogas premixed charge diesel dual fuelled engine. *Energy Convers Manage* 2007;48:2286–308. <https://doi.org/10.1016/j.enconman.2007.03.020>.
- [21] Pattanaik BP, Nayak C, Nanda BK. Investigation on utilization of biogas & Karanja oil biodiesel in dual fuel mode in a single cylinder DI diesel engine n.d.;12.
- [22] Swami Nathan S, Mallikarjuna JM, Ramesh A. An experimental study of the biogas–diesel HCCI mode of engine operation. *Energy Convers Manage* 2010;51:1347–53. <https://doi.org/10.1016/j.enconman.2009.09.008>.
- [23] Henham A, Makkar MK. Combustion of simulated biogas in a dual-fuel diesel engine. *Energy Convers Manage* 1998;39:2001–9.
- [24] Ramesha DK, Bangaria AS, Rathod CP, Samarth Chaitanya R. Combustion, performance and emissions characteristics of a biogas fuelled diesel engine with fish biodiesel as pilot fuel. *Biofuels* 2015;6:9–19. <https://doi.org/10.1080/17597269.2015.1036960>.
- [25] Ramesha DK, Bangaria AS, Chirag PR, Chaitanya RS. Experimental investigation of biogas-biodiesel dual fuel combustion in a diesel engine. *J Middle Eur Constr Des* 2015;13:12–20.
- [26] Kalsi SS, Subramanian KA. Effect of simulated biogas on performance, combustion and emissions characteristics of a bio-diesel fueled diesel engine. *Renew Energy* 2017;106:78–90. <https://doi.org/10.1016/j.renene.2017.01.006>.
- [27] Bora BJ, Saha UK. Improving the performance of a biogas powered dual fuel diesel engine using emulsified rice bran biodiesel as pilot fuel through adjustment of compression ratio and injection timing. *J Eng Gas Turbines Power* 2015;137. <https://doi.org/10.1115/1.4029708>. 091505–091505–14.
- [28] Bora BJ, Saha UK. Comparative assessment of a biogas run dual fuel diesel engine with rice bran oil methyl ester, pongamia oil methyl ester and palm oil methyl ester as pilot fuels. *Renew Energy* 2015;81:490–8. <https://doi.org/10.1016/j.renene.2015.03.019>.
- [29] Weiland P. Biogas production: current state and perspectives. *Appl Microbiol Biotechnol* 2010;85:849–60. <https://doi.org/10.1007/s00253-009-2246-7>.
- [30] Murto M, Björnsson L, Mattiasson B. Impact of food industrial waste on anaerobic co-digestion of sewage sludge and pig manure. *J Environ Manage* 2004;70:101–7. <https://doi.org/10.1016/j.jenvman.2003.11.001>.
- [31] Comino E, Riggio VA, Rosso M. Biogas production by anaerobic co-digestion of cattle slurry and cheese whey. *Bioresour Technol* 2012;114:46–53. <https://doi.org/10.1016/j.biortech.2012.02.090>.
- [32] Neshat et al. – 2017 – Anaerobic co-digestion of animal manures and ligno.pdf n.d.
- [33] Valenti et al. 2018 – Anaerobic co-digestion of multiple agricultural re.pdf n.d.
- [34] Jurado et al. – 2016 – Continuous anaerobic digestion of swine manure AD.pdf n.d.
- [35] Andriamanohiarisoamanana et al. – 2017 – Anaerobic co-digestion of dairy manure, meat and b.pdf n.d.
- [36] Ning et al. – 2019 – Simultaneous biogas and biogas slurry production f.pdf n.d.
- [37] ADEME-2011 Méthanisation à la ferme.pdf n.d.
- [38] Yusri IM, Abdul Majeed APP, Mamat R, Ghazali MF, Awad OI, Azmi WH. A review on the application of response surface method and artificial neural network in engine performance and exhaust emissions characteristics in alternative fuel. *Renew Sustain Energy Rev* 2018;90:665–86. <https://doi.org/10.1016/j.rser.2018.03.095>.
- [39] Wong KI, Wong PK, Cheung CS, Vong CM. Modelling of diesel engine performance using advanced machine learning methods under scarce and exponential data set. *Appl Soft Comput* 2013;13:4428–41. <https://doi.org/10.1016/j.asoc.2013.06.006>.
- [40] Abd Alla GH, Soliman HA, Badr OA, Abd Rabbo MF. Combustion quasi-two zone predictive model for dual fuel engines. *Energy Convers Manage* 2001;42:1477–98. [https://doi.org/10.1016/S0196-8904\(00\)00143-6](https://doi.org/10.1016/S0196-8904(00)00143-6).
- [41] Soyhan HS, Yasar H, Walmsley H, Head B, Kalghatgi GT, Sorusbay C. Evaluation of heat transfer correlations for HCCI engine modeling. *Appl Therm Eng* 2009;29:541–9. <https://doi.org/10.1016/j.applthermaleng.2008.03.014>.
- [42] Aklouche FZ, Loubar K, Bentebbiche A, Awad S, Tazerout M. Predictive model of the diesel engine operating in dual-fuel mode fuelled with different gaseous fuels. *Fuel* 2018;220:599–606. <https://doi.org/10.1016/j.fuel.2018.02.053>.
- [43] Dibakor Boruah, Pintu Kumar Thakur, Dipal Baruah, University of Sussex, UK; and Gauhati University (GIMT-Tezpur), India. Artificial Neural Network based Modelling of Internal Combustion Engine Performance. *International Journal of Engineering Research And* 2016;V5. <https://doi.org/10.17577/IJERTV5IS030924>.
- [44] Garg AB, Diwan P, Saxena M. Artificial Neural Networks based Methodologies for Optimization of Engine Operations 2012;3:5.
- [45] Rida A, Nahim HM, Younes R, Shraim H, Ouladsine M. Modeling and simulation of the thermodynamic cycle of the diesel engine using neural networks. *IFAC-PapersOnLine* 2016;49:221–6. <https://doi.org/10.1016/j.ifacol.2016.07.037>.
- [46] Experimental study and prediction of the performance and exhaust emissions of mixed Jatropha curcas-Ceiba pentandra biodiesel blends in diesel engine using artificial neural networks | Elsevier Enhanced Reader n.d. <https://doi.org/10.1016/j.jclepro.2017.06.065>.
- [47] Modeling of a dual fueled diesel engine operated by a novel fuel containing glycerol triacetate additive and biodiesel using artificial neural network tuned by genetic algorithm to reduce engine emissions | Elsevier Enhanced Reader n.d. <https://doi.org/10.1016/j.energy.2018.11.142>.
- [48] Modeling of a dual fueled diesel engine operated by a novel fuel containing glycerol triacetate additive and biodiesel using artificial neural network tuned by genetic algorithm to reduce engine emissions | Elsevier Enhanced Reader n.d. <https://doi.org/10.1016/j.energy.2018.11.142>.
- [49] Application of artificial intelligence (AI) in characterization of the performance-emission profile of a single cylinder CI engine operating with hydrogen in dual fuel mode: An ANN approach with fuzzy-logic based topology optimization | Elsevier Enhanced Reader n.d. <https://doi.org/10.1016/j.ijhydene.2016.07.016>.
- [50] Experimental and artificial neural network approach of noise and vibration characteristic of an unmodified diesel engine fuelled with conventional diesel, and biodiesel blends with natural gas addition | Elsevier Enhanced Reader n.d. <https://doi.org/10.1016/j.fuel.2017.01.113>.
- [51] Artificial Neural Network modeling of a hydrogen dual fueled diesel engine characteristics: An experiment approach | Elsevier Enhanced Reader n.d. <https://doi.org/10.1016/j.ijhydene.2017.04.096>.
- [52] Pyle D. Data preparation for data mining. 1st ed. San Francisco, CA, USA: Morgan Kaufmann Publishers Inc.; 1999.
- [53] Zhao Y, Sun F, Yu J, Cai Y, Luo X, Cui Z, et al. Co-digestion of oat straw and cow manure during anaerobic digestion: stimulative and inhibitory effects on fermentation. *Bioresour Technol* 2018;269:143–52. <https://doi.org/10.1016/j.biortech.2018.08.040>.
- [54] Uzun A. Air mass flow estimation of diesel engines using neural network. *Fuel* 2014;117:833–8. <https://doi.org/10.1016/j.fuel.2013.09.078>.
- [55] Arrêté du 13 décembre 2016 n.d. <https://www.legifrance.gouv.fr/affichTexte.do?cidTexte=JORFTEXT000033585226&categorieLien=id> (accessed March 14, 2019).
- [56] Sombatwong P, Thaiyasuit P, Pianthong K. Effect of pilot fuel quantity on the performance and emission of a dual producer gas-diesel engine. *Energy Procedia* 2013;34:218–27. <https://doi.org/10.1016/j.egypro.2013.06.750>.
- [57] Wei L, Geng P. A review on natural gas/diesel dual fuel combustion, emissions and performance. *Fuel Process Technol* 2016;142:264–78. <https://doi.org/10.1016/j.fuproc.2015.09.018>.
- [58] Aklouche FZ, Loubar K, Bentebbiche A, Awad S, Tazerout M. Experimental investigation of the equivalence ratio influence on combustion, performance and exhaust emissions of a dual fuel diesel engine operating on synthetic biogas fuel. *Energy Convers Manage* 2017;152:291–9. <https://doi.org/10.1016/j.enconman.2017.09.050>.
- [59] Jiaqiang E, Zhao X, Qiu L, Wei K, Zhang Z, Deng Y, et al. Experimental investigation on performance and economy characteristics of a diesel engine with variable nozzle turbocharger and its application in urban bus. *Energy Convers Manage* 2019;193:149–61. <https://doi.org/10.1016/j.enconman.2019.04.062>.
- [60] Barik D, Murugan S. Investigation on combustion performance and emission characteristics of a DI (direct injection) diesel engine fueled with biogas–diesel in dual fuel mode. *Energy* 2014;72:760–71. <https://doi.org/10.1016/j.energy.2014.11.142>.

- 05.106.
- [61] Heywood JB. *Internal combustion engine fundamentals*. New York: McGraw-Hill; 1988.
- [62] US EPA O. CHP Benefits. US EPA 2015. <https://www.epa.gov/chp/chp-benefits> (accessed December 6, 2019).
- [63] Teymoori Hamzehkolaei F, Amjady N. A techno-economic assessment for replacement of conventional fossil fuel based technologies in animal farms with biogas fueled CHP units. *Renew Energy* 2018;118:602–14. <https://doi.org/10.1016/j.renene.2017.11.054>.
- [64] 8 to 340 kW vegetable oil-fired ecoGEN CHP units. Innovative micro- and mini-CHPs that run on vegetable oil | CogenGreen n.d. <https://www.cogengreen.com/en/8-340-kw-vegetable-oil-fired-ecogen-chp-units-innovative-micro-and-mini-chps-run-vegetable-oil> (accessed November 4, 2019).